JACC: CARDIOVASCULAR INTERVENTIONS
VOL. 7, NO. 9, 2014

ISSN 1936-8798/$36.00
PUBLISHED BY ELSEVIER INC.
http://dx.doi.org/10.1016/j.jcin.2014.04.009

Real-Time Assessment of Myocardial Viability in the Catheterization Laboratory Using the Intracoronary Electrograms Recorded by the PTCA Guidewire in Patients With Left Ventricular Dysfunction

Comparison With Delayed-Enhancement Magnetic Resonance Imaging

Ettore Petrucci, MD,* Vruyr Balian, MD,* Andrea Bocchieri, PhD†

ABSTRACT

OBJECTIVES This study aimed to determine whether the intracoronary electrograms (IC-EGMs) recorded using a standard percutaneous coronary intervention guidewire could provide myocardial viability information.

BACKGROUND The revascularization of dysfunctional but viable myocardium may confer prognostic benefits compared with medical therapy in patients with post-ischemic heart failure. However, knowledge of myocardial viability is often unavailable at the time of the procedure.

METHODS The peak-to-peak voltage of 317 IC-EGMs recordings from 25 patients with a previous myocardial infarction and systolic dysfunction were matched with corresponding delayed-enhancement magnetic resonance imaging sites using a 17-segment model of the left ventricle.

RESULTS Sixty-seven recordings were obtained from segments classified as complete scar on delayed-enhancement magnetic resonance imaging (group A), 162 from partially viable segments (group B), and 88 from fully viable segments (group C). Three high-pass (HP) filters (0.5, 30, and 100 Hz) were applied to the signals to modulate their spatial resolution. For all filters, the peak-to-peak voltage significantly decreased from group C to group B to group A ($p < 0.001$ for all comparisons). When receiver-operating characteristic analysis was used to compare nonviable (group A) with viable (group B + C) segments, the optimal discriminating voltages were 4.6, 2.2, and 0.78 mV for, respectively, HP-0.5, HP-30, and HP-100 filters, with a sensitivity of 92%, 94%, and 99% and a specificity of 70%, 79%, and 69%.

CONCLUSIONS The amplitude of the IC-EGMs discriminates viable from nonviable left ventricular segments. Because this technique is simple and inexpensive and provides real-time results, it is potentially useful to aid decision making in the catheterization laboratory. (J Am Coll Cardiol Intv 2014;7:988–96) © 2014 by the American College of Cardiology Foundation.

The revascularization of dysfunctional but viable myocardium may improve left ventricular (LV) function and may confer prognostic benefits compared with medical therapy in patients with post-ischemic heart failure (1-3). Therefore, knowledge of tissue viability is an important factor in the decision-making process during percutaneous coronary interventions (PCIs) in these patients (4). Due to the low accuracy of electrocardiography Q waves and basal echocardiography (5,6), more

From *Cardiologia Interventistica, Ospedale di Busto Arsizio, Busto Arsizio, Italy; and †Ingegneria Clinica, Ospedale di Busto Arsizio, Busto Arsizio, Italy, and Dipartimento di Informatica e Sistemistica, Facoltà di Bioingegneria, Università di Pavia, Pavia, Italy. The authors have reported that they have no relationships relevant to the contents of this paper to disclose.

Manuscript received December 31, 2013; revised manuscript received March 13, 2014, accepted April 11, 2014.

sophisticated techniques such as dobutamine stress echocardiography, rest-redistribution perfusion scan, positron emission tomography, and delayed-enhancement magnetic resonance imaging (DE-MRI) (2,7) are currently used to assess myocardial viability, but they cannot be performed online in the catheterization laboratory.

Because scarred regions are electrically silent, evaluation of myocardial electrical activity has been proposed as an alternative method to assess viability. Systematic experimental (8,9) and clinical (10–13) studies have demonstrated that endocardial and epicardial electrograms can reliably differentiate dense scar from hibernating and normal myocardium on the basis of reduced voltage, longer duration, and fractionation. Electroanatomic voltage maps are currently used to guide the substrate-based ablation of ventricular tachycardia in patients with structural heart disease (14). Although accurate and able to provide real-time data, these complex and time-consuming catheter-based techniques are inappropriate for use in a routine PCI procedure.

SEE PAGE 997

This study was designed to assess whether the correlation between viability and electrical activity could be demonstrated using a standard PCI guidewire as an exploring electrode, allowing the operator to quickly assess myocardial tissue viability in real time without adding complexity, time, costs, and risks to the procedure. To evaluate this hypothesis, we correlated the peak-to-peak voltage of appropriately recorded and processed intracoronary electrograms (IC-EGMs) with DE-MRI images obtained from the same segment (15) of the left ventricle in a population of consecutive patients with previous myocardial infarction (MI), multivessel coronary artery disease, and impaired systolic function undergoing elective PCI.

METHODS

POPULATION. Clinically stable patients with echocardiographic left ventricular ejection fraction (LVEF) <40% who were scheduled to undergo an electively staged procedure in a nonculprit vessel 6 to 8 weeks after primary PCI for an ST-segment elevation MI were eligible for enrollment in the study. Patients with claustrophobia, implantable cardiac devices, impaired renal function, atrial fibrillation, and LV thrombus were excluded. The study protocol was approved by the local Ethics Committee for Human Research. Informed consent was obtained from all patients. All patients underwent a full cardiac DE-MRI study during the same hospital admission ±3 days before the planned PCI.

PCI AND IC-EGM RECORDINGS. PCIs were performed according to standard clinical practice via femoral or radial access. To reduce the effective electrode size and therefore the field of view of the intracoronary lead (16), the guidewire (Hi-Torque Balance Middleweight, Guidant Vascular Intervention, Temecula, California) was electrically insulated with a microcatheter (FineCross MG, Terumo, Tokyo, Japan), leaving only the distal 5 mm of the radiopaque tip uninsulated (**Figure 1**). IC-EGMs were recorded at ~2-cm intervals within the recent (and remote in 4 patients) infarct-related artery and the elective PCI artery and their suitable branches. Low-voltage intrastent signals were excluded. Annular positions (where an atrial wave was recorded) were also excluded because our experience (**Figure 2**) and previous studies demonstrated that electrograms recorded at these sites are unreliable for viability assessment due to the presence of fibrous tissue, epicardial fat (17), and fiber orientation (12).

Each recording site was assigned to 1 segment of the 17-segment model of the left ventricle (15) after offline analysis of 2 orthogonal projections of the guidewire position, matched with 2 ventriculography images using exactly the same orientation and distance of the image intensifier (**Figure 1**).

MAGNETIC RESONANCE IMAGING. A 1.5-T magnetic resonance imaging scanner (Magnetom Avanto, Siemens, München, Germany) with a cardiac software package was used for imaging. The following electrocardiography-gated cine images were acquired before and 15 min after the infusion of gadolinium diethylenetriamine tetraacetic acid (0.2 mmol/kg): 2-chamber-long axis, 4-chamber-long axis, and a short-axis stack covering the entire left ventricle from the base to apex.

The freely available Segment software version 1.8 R1405 (Medviso, Lund, Sweden) (18) was used for segmentation and analysis of short-axis slices. The Segment automatic weighted tool was used to quantify hyperenhanced regions (**Figure 3**, left) in terms of area (percentage of the segment area satisfying the scar criteria) and transmurality (maximal percentage of wall thickness satisfying the scar criteria). Values from slices assigned to the same segment were averaged. Because standard criteria for automatic scar definition are still lacking (19), images were also reviewed by an expert

ABBREVIATIONS AND ACRONYMS

DE-MRI = delayed-enhancement magnetic resonance imaging

HP = high pass

IC-EGM = intracoronary electrogram

LV = left ventricular

LVEF = left ventricular ejection fraction

MI = myocardial infarction

PCI = percutaneous coronary intervention

ROC = receiver-operating characteristic

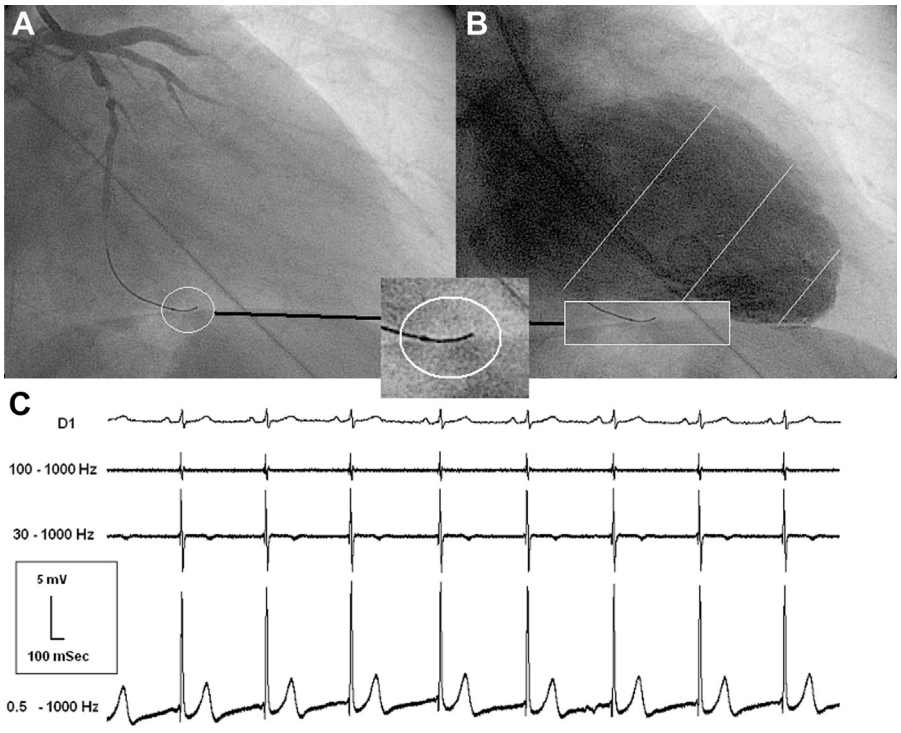

FIGURE 1 Overview of the Intracoronary Electrogram Recording Technique

The guidewire tip, protruding from the insulating microcatheter in 45° right anterior oblique projection **(A)**, is superimposed on a left ventriculogram obtained with exactly the same orientation and distance of the image intensifier, resulting in a mid-ventricular position **(B)**. Since in the 45° left anterior oblique projection (not shown), the position was at 6 o'clock, the site was assigned to segment 10 (mid-inferior) of the 17-segment model. **(C)** The recorded signals are displayed as they appear on the screen in real time (from top to bottom, the surface lead D1 and the intracoronary electrocardiograms high-pass filtered at 100, 30, and 0.5 Hz).

operator (unaware of the automated results) and classified as hyperenhanced (complete scar), not hyperenhanced (no scar present), or intermediate. The final classification of each segment (Figure 3, right) was obtained as follows: 1) group A, transmural scar, scar area >75%, scar transmurality >75% and defined as complete transmural scar by the expert operator; 2) group B, partially viable, all segments not fulfilling the group A criteria and the group C criteria, including segments with nontransmural scar, encompassing the infarction border zone and with discordance between automatic and visual assessment; and 3) group C, fully viable, scar area <25%, scar transmurality <25% and defined as not hyperenhanced myocardium by the expert operator.

IC-EGMS FILTERING AND PROCESSING. IC-EGMs were recorded by connecting the proximal tip of the guidewire (exploring electrode) to the positive input, and a skin electrode placed over the left iliac crest (reference or indifferent electrode) with the negative input of the recording amplifier (Signal Acquisition Module 8300, Boston Scientific Model, Natick, Massachusetts). The amplifier was set to the bipolar configuration; however, due to the distance between the exploring and reference electrodes, the recorded signal was, in fact, unipolar (20). After analog-to-digital conversion (sampling rate, 3000 samples per second; discretization, 6.25 μV), 3 digital bandpass filters were applied. The first, high-pass (HP) limit of 0.5 Hz (HP-0.5), resulted in a minimally filtered signal containing high (near-field) and low (far-field) frequency components. The second, HP limit of 30 Hz (HP-30), and the third, HP limit of 100 Hz (HP-100), progressively reduced the low-frequency (far-field) components, improving the detection of lower amplitude local signals from abnormal regions (16,20). For all filters, the low-pass limit was set at 1,000 Hz.

The field of view of our intracoronary lead was empirically assessed by evaluating the contribution of the well-separated atrial and ventricular waves during the withdrawal of the guidewire from the basal left ventricle to the aortic root. Figure 2 shows that sites (either atrial or ventricular) farther than 10 to 15 mm from the exploring electrode have only a slight influence on the HP-0.5 signal and do no affect the HP-30 and particularly the HP-100 signals. Such a high spatial resolution could not be obtained using other recording techniques (unipolar configuration, standard electrocardiographic surface filters and uninsulated guidewire) that we tested in the preliminary phase of this study.

Custom software was developed to calculate the peak-to-peak amplitude in millivolts for each recording site and for each filter. Data from 3 consecutive stable (interbeat variability <10%) sinus beats were averaged to obtain the final value used in the analysis.

STATISTICAL ANALYSIS. The mean and SD of the peak-to-peak voltage were calculated for each group and for each filter. No corrections were made for multiple IC-EGM assessments within individuals. The difference among the 3 groups was assessed using 2-tailed analysis of variance and, if the null hypothesis was rejected, with a Student *t* test between paired groups (A vs. B, A vs. C, and B vs. C), without adjustment for multiplicity.

Receiver-operating characteristic (ROC) analysis was performed using the MATLAB 7.13 R2011b software (MathWorks Inc., Natick, Massachusetts). Because the likely real-world application would be the revascularization of any viable tissue, we merged groups B and C (viable myocardium present) and compared them with group A (transmural scar, revascularization unlikely to improve heart function), calculating sensitivity and false positive rate (1-specificity) for viability detection over the full range of voltages. Sensitivity is the fraction of the true viable segments that are correctly detected and the false positive rate is the fraction of the true nonviable segments that are falsely classified as viable.

For each filter, the area under the curve was calculated to express the overall performance. In addition, the performance was calculated at 2 relevant operating points: 1) the point allowing the maximal viability specificity while the sensitivity is 100% (i.e., the lowest voltage of the viable group distribution); and 2) the optimal operating point of the ROC curve (the closest to the upper left corner), calculated using the MATLAB function OPTROCPT.

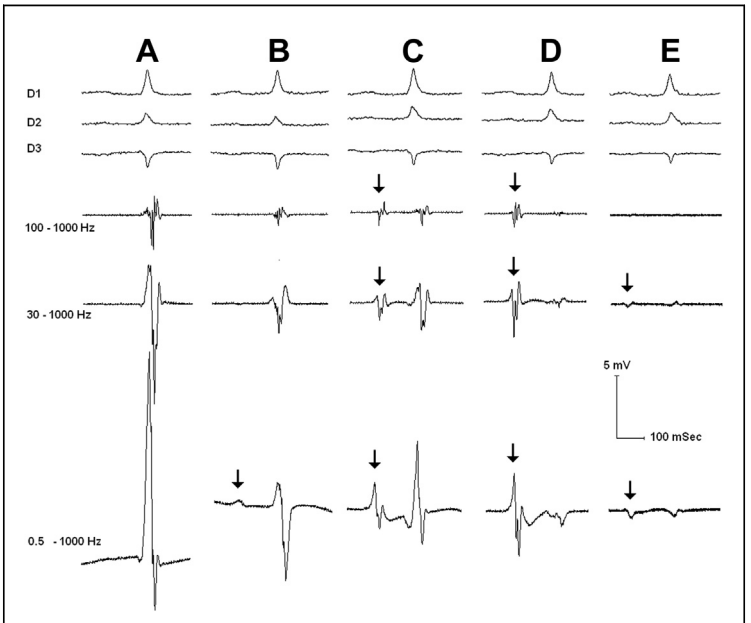

FIGURE 2 Serial Intracoronary Recordings During Withdrawal of the Guidewire From the Basal Left Ventricle to the Aortic Root

From **top to bottom**, 3 surface electrocardiography leads and the intracoronary electrograms high-pass (HP) filtered at 100, 30, and 0.5 Hz are displayed. The **vertical arrows** indicate the atrial component. **(A)** In the proximal obtuse marginal branch, 20 mm away from the ostium, only a large ventricular wave is recorded. **(B)** When the guidewire tip is ~10 to 15 mm distal to the annulus, a small far-field atrial wave appears in HP-0.5 signal, whereas the ventricular wave voltage decreases. **(C)** Moving the guidewire in the atrioventricular groove (circumflex artery), the atrial component becomes well evident and spiky (near-field) with all filters. **(D)** In the left main coronary artery, close to the atrial appendages (where the highest atrial voltages are usually recorded endocardially), the atrial wave reaches its maximal amplitude and the atrial/ventricular ratio is >1 with all filters, whereas the ventricular wave further decreases and is barely visible on the HP-100 signal. **(E)** Finally, when the guidewire is floating in the aortic root at the level of the sinotubular junction, only small and slurred (far-field) atrial and ventricular waves are recorded in HP-0.5 and HP-30, and no electrical activity at all in HP-100 signals.

RESULTS

Twenty-five consecutive patients fulfilling the inclusion criteria were included. The age (mean ± SD) was 64 ± 12 years, 20 (80%) were male, 12 (48%) had hypertension, 4 (16%) were diabetic, 10 (40%) were dyslipidemic, and 11 (44%) had a family history of coronary artery disease. The location of the recent infarct was anterior in 22 (88%) and inferior in 3 (12%), whereas a history of remote MI was reported in 4 patients, anterior in 2, and inferior in 2. The LVEF was 33 ± 5%.

Overall, 317 intracoronary recordings (average, 12 recordings/patient; range, 7 to 18) were available for analysis. Of these, 67 (21%) were recorded from

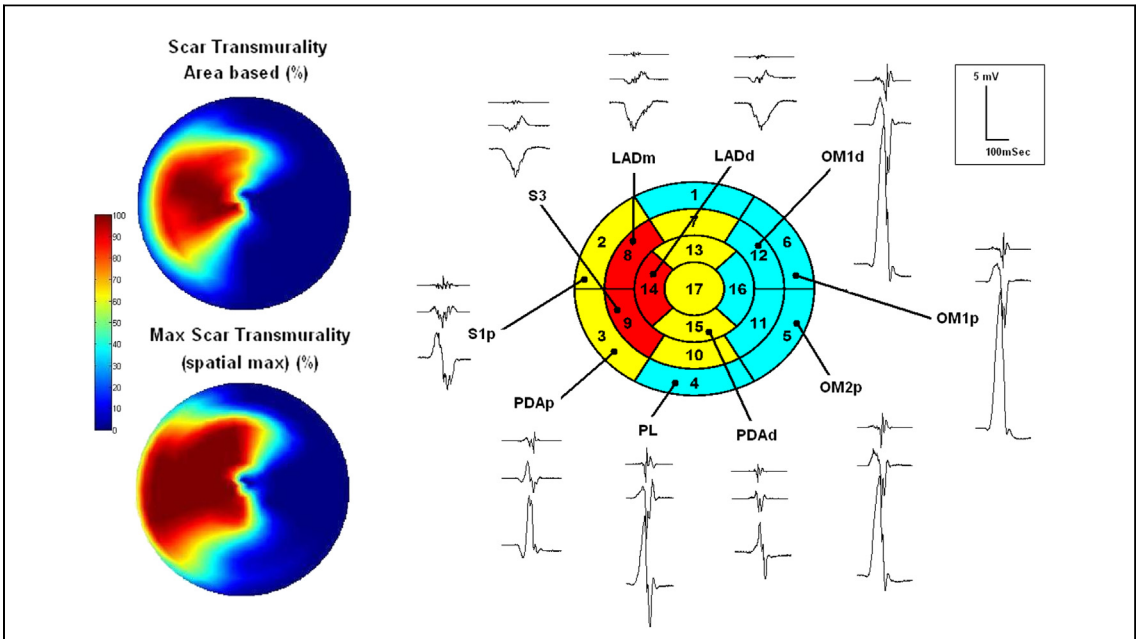

FIGURE 3 DE-MRI Viability Study and Intracoronary Recordings Obtained 2 Months After a Primary PCI of the Proximal LAD Artery for an Anterior ST-Segment Elevation Acute MI

The patient was scheduled for a staged procedure of a critical stenosis of the proximal right coronary artery. The **2 bull's eye plots on the left** (scar transmurality area based **[top]** and maximal scar transmurality **[bottom]**) show the results provided by the automatic analysis of DE-MRI. They were merged with visual analysis results to obtain the polar plot represented on the **right**, in which each segment is classified as complete scar (group A, **red**), partially viable (group B, **yellow**), or fully viable (group C, **blue**). Selected recordings are shown around the polar map, linked with the left ventricular segment and the vessel from which they were recorded (**top to bottom**: the IC-EGMs HP-filtered at 100, 30, and 0.5 Hz). High voltages are recorded in the fully viable lateral wall, whereas very low signals are found in the scarred mid-apical septum, with fractionation in HP-100 and HP-30, and QS morphology in HP-0.5 signals. The inferior wall and the basal inferior septum, sampled through the PDA beyond the critical stenosis, show intermediate voltages in the partially viable range, in agreement with DE-MRI results. DE-MRI = delayed-enhancement magnetic resonance imaging; D = diagonal; d = distal; HP = high pass; LAD = left anterior descending; m = mid; OM = obtuse marginal; PDA = posterior descending artery; PL = posterolateral; p = proximal; S = septal; 1 = first branch; 2 = second branch; 3 = third branch.

segments classified as complete scar (group A) by DE-MRI, 162 (51%) from partially viable segments (group B), and 88 (28%) from fully viable segments (group C). Their topographic distribution in the 17-segment model of the left ventricle is shown in Table 1. The angiographic recording sites were in the left anterior descending artery in 112 samples, diagonal branches in 66, septal branches in 37, obtuse marginal branches in 75, posterior descending artery in 22, and posterolateral branches in 6 (however, it is worth noting that the explored vessel is not relevant in this context because the same segment can sometimes be sampled using different branches, depending on coronary anatomy [21]).

High-quality, noise-free, and stable signals were consistently obtained using our recording technique (Figure 1).

COMPARISON OF IC-EGMS IN SCARRED, PARTIALLY VIABLE, AND FULLY VIABLE SEGMENTS. The mean ± SD of the peak-to-peak voltage for groups A, B, and C and for the 3 filters are reported in Table 2. For all filters, the voltage decreases from group C to group B to group A, with high statistical significance ($p < 0.0001$) for all comparisons (analysis of variance and Student *t* test).

An example of recordings from complete scar (group A) and fully viable site (group C) in the same patient is represented in Figure 4. HP filtering reduces the IC-EGM amplitude in both normal and scarred tissue. With all filter settings, the amplitude of the scar electrogram is very low compared with the fully viable electrogram. Moreover, the scar IC-EGM has a qR configuration in the HP-0.5 signal, indicating that the electrical wavefront spreads away from the site and is

TABLE 1 Topographic Distribution of the Intracoronary Recording Sites According to the 17-Segment Model of the Left Ventricle

Location	Anterior 42 (6/19/17)	Anteroseptal 79 (17/45/17)	Inferoseptal 60 (16/35/9)	Inferior 24 (5/15/4)	Inferolateral 49 (6/25/18)	Anterolateral 40 (8/13/19)
Basal 73 (12/27/34)	S1 12 (2/3/7)	S2 16 (3/5/8)	S3 14 (2/8/4)	S4 2 (0/2/0)	S5 13 (0/5/8)	S6 16 (5/4/7)
Mid-cavity 149 (25/85/39)	S7 30 (4/16/10)	S8 39 (7/27/5)	S9 21 (6/13/2)	S10 12 (3/7/2)	S11 23 (2/13/8)	S12 24 (3/9/12)
Apical 72 (21/40/11)		Anterior	Septal	Inferior	Lateral	
		S13 24 (7/13/4)	S14 25 (8/14/3)	S15 10 (2/6/2)	S16 13 (4/7/2)	
Apex			S17 23 (9/10/4)			

For each segment, row, and column, the total number of samples and, in parentheses, the number of samples for groups A (scar), B (partially viable), and C (fully viable) are reported.
S1 through S17 = left ventricular segments.

prolonged and fragmented in the HP-100 signal, suggesting slow and anisotropic conduction; although fractionation is difficult to quantify (9), our preliminary experience suggests that it is always present in HP-filtered IC-EGMs recorded from abnormal myocardium (Figure 3).

ROC ANALYSIS AND CUTOFF THRESHOLDS FOR VIABILITY DETECTION. The ROC curves comparing the peak-to-peak voltage in partially or fully viable (groups B + C) versus nonviable (group A) segments are shown Figure 5. The areas under the curve (95% confidence interval) are 92% (90% to 95%), 94% (90% to 97%), and 93% (91% to 96%), respectively, for the HP-0.5, HP-30, and HP-100 filters, with no statistical difference between the curves (p = NS). Table 3 shows the performance of the 3 filters for the 2 pre-specified operating points and the corresponding voltage cutoffs for detection. When the operating point is set equal to the minimal voltage of the viable (B + C) group distribution, representing the best specificity while sensitivity is still 100% (no viable segment is misclassified), the HP-100 filter is clearly superior; the optimal operating point (less influenced by outliers) provides more balanced results, with the HP-30 filter performing slightly better.

DISCUSSION

MAIN FINDINGS. 1) The local IC-EGM voltage can identify LV segments classified as transmural scar, partially viable, and fully viable by DE-MRI. In addition, voltage thresholds are provided to accurately detect LV segments containing viable tissue. 2) This technique can be applied using a standard PCI guidewire and therefore has the potential to aid the decision-making process of the operator in real time.

EFFECT OF FILTERING. The 3 filters provide similar accuracy in differentiating groups A, B, and C, suggesting a compromise between surface and transmural performance. However, when assessing the mere presence/absence of viable tissue (a more clinically oriented endpoint), the more localized HP-filtered signals provide slightly better results (Table 3). This can be explained taking into account the epicardial position of the intracoronary electrode, the field of view of the 3 filters, and the transmural distribution of the post-infarction scar, which spreads from the subendocardium, which is always involved, to the subepcardium, which can be spared (10,19). Further studies are needed to assess the clinical relevance of these observations and to clarify whether other more filter-specific features (maximal negative slope and Q waves for minimally filtered signals and duration and fractionation for HP-filtered signals) may improve the characterization of the mapped substrate (8,9).

It is also noteworthy that HP filtering reduces the overall voltage, making the thresholds proposed in this work reproducible only by using the same filters.

PREVIOUS WORK. The technique of pacing and sensing the left ventricle using an intracoronary guidewire was first introduced in clinical medicine in

TABLE 2 Peak-to-Peak Voltage of Intracoronary Electrograms in Group A (Scar), B (Partially Viable), and C (Fully Viable) With Different Filter Settings

Filter	Group A (n = 67)	Group B (n = 162)	Group C (n = 88)	F Value (ANOVA)	p Value* (ANOVA)
HP-100	0.75 ± 0.45	1.93 ± 1.08	3.26 ± 1.48	88.3	<0.0001
HP-30	1.78 ± 0.92	4.42 ± 1.91	7.01 ± 2.2	134.0	<0.0001
HP-0.5	3.96 ± 1.74	8.49 ± 3.6	13.37 ± 3.82	121.0	<0.0001

Values (in millivolts) are mean ± SD. *Student *t* test between pairs of groups: p < 0.0001 for all comparisons.
ANOVA = analysis of variance; HP = high pass.

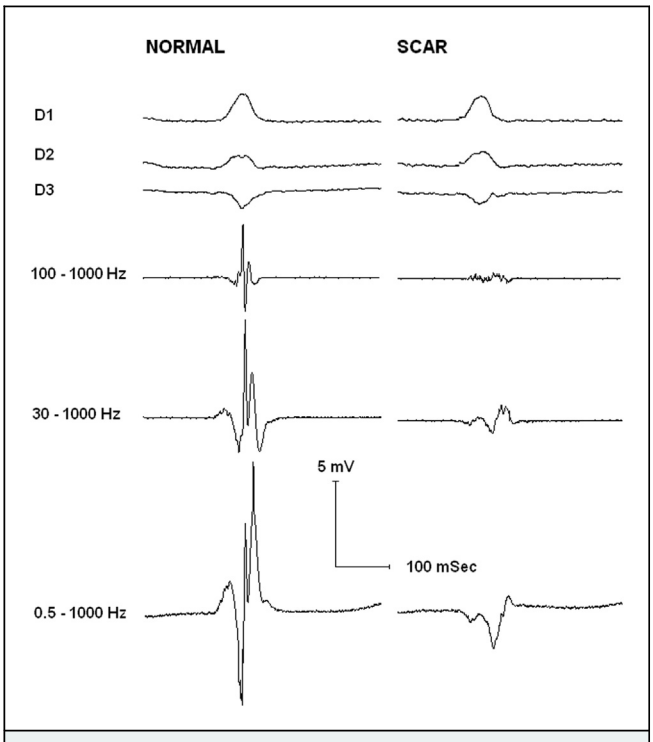

FIGURE 4 Intracoronary Recordings From Fully Viable Myocardium and Transmural Scar in a Patient With a Previous Anterior Myocardial Infarction

From **top to bottom**, 3 surface electrocardiography leads and the HP-filtered IC-EGMs are displayed. For all filters, the voltage of the scar signal **(right panel)** is very low compared with the fully viable site **(left panel)**. Note also the qR morphology of the HP-0.5 signal and the fractionation of the HP-100 signal in scar recordings. HP = high pass; IC-EGMs = intracoronary electrograms.

1985 (22). More recently, the IC-ECG has been demonstrated to be useful to predict myocardial recovery after primary (23,24) or elective (25) angioplasty, to assess periprocedural myocardial damage (26,27), to detect myocardial ischemia during adenosine infusion (28), and to evaluate the protective power of collaterals in terms of preserving myocardium or life (29). These studies were performed using standard unipolar electrocardiography leads (low-pass filtered) and focusing on transient ST-segment shift. Intracoronary mapping with a PCI guidewire has been anecdotally reported in the setting of epicardial ventricular tachycardia ablation (30). To our knowledge, this is the first study evaluating the IC-EGM voltage to assess myocardial viability during PCI in humans.

SEGMENT-BASED APPROACH VERSUS THE CLINICAL DECISION-MAKING PERSPECTIVE. Although standard LV segmentation provides a useful framework to match angiographic recording sites with the corresponding DE-MRI segments, the complex relationships between dysfunctional LV areas and coronary anatomy should be considered from a clinical perspective (21).

This technique cannot be applied in the presence of complete coronary occlusions, unless easily accessible collaterals reaching the region of interest are available for mapping.

In nonoccluded lesions, if voltages exceeding the scar threshold are recorded from the post-stenotic main vessel (which is usually in the center of the necrotic or damaged area, minimizing the risk of measuring potentials of adjacent nonaffected vessel areas), viability is confirmed and no further mapping is required. Because this information is obtained in real time by simply connecting the guidewire with the recording system, the technique is very cost-effective in these cases. Conversely, if only low-voltage, fractionated signals are consistently recorded from the post-stenotic main vessel, the operator should try to map the whole region of interest through all the suitable branches and collaterals to exclude significant residual viability in the border zone. If this approach (which requires a favorable coronary anatomy, time, and skill) should prove to be feasible, the technique could also be useful to avoid (or postpone) revascularization, preventing unnecessary, costly, and sometimes risky procedures (for example, a widely patent collateral branch supplying a viable bed can be occluded after stenting a main branch stenosis supplying a necrotic area).

STUDY LIMITATIONS. Our definition of groups A, B, and C is arbitrary because no standard criteria are available so far for quantitative DE-MRI analysis (19). Moreover, we cannot exclude a possible mismatch between DE-MRI and angiographic segmentation.

No attempt was made to systematically map the LV epicardial surface because a complete map is not required for clinical decision making. Clearly, coronary anatomy can limit adequate mapping. In the presence of complete coronary occlusion and the absence of collateral vessels, the region of interest cannot be sampled. Therefore, the technique is suggested only for easily passable coronary lesions supplying dysfunctional LV regions.

Because only patients with reduced LVEF were included in the study, there is a prevalence of anteroseptal wall scars and a fewer inferior and lateral wall scars. Basal segments are also underrepresented due to the exclusion of the recordings containing an atrial signal.

The assessment of the coronary wall anatomy (using intravascular ultrasound or coronary computed

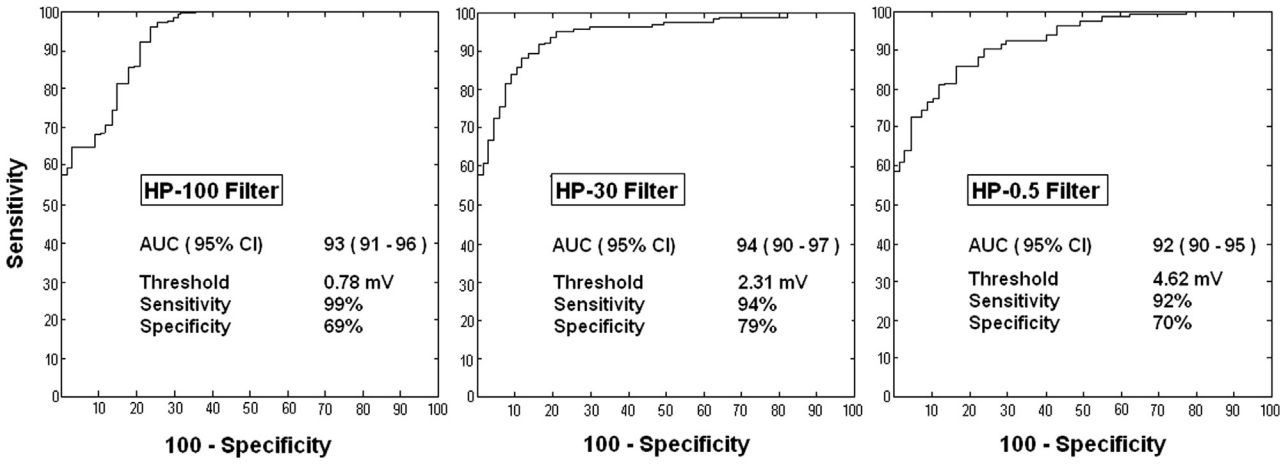

FIGURE 5 Receiver-Operating Characteristic Curves Comparing the Peak-to-Peak Voltage of Intracoronary Electrograms in Viable and Complete Scar Segments With Different Filter Settings

For the 3 filters, the AUC, and the characteristics of the "optimal" operating point are reported. AUC = area under the curve; CI = confidence interval; HP = high pass.

tomography angiography) was not performed in our patients; therefore, the influence of arterial wall abnormalities on IC-EGMs was not evaluated. Although calcium or perivascular fat might act as electrical insulators reducing intracoronary voltages, multiple recordings from contiguous sites and the evaluation of signal morphology (fractionation) should permit the differentiation from true scar tissue.

CONCLUSIONS

This investigation evaluated the use of the local systolic IC-EGMs to assess myocardial tissue viability in real time, providing information in patients with LV dysfunction in whom an imaging viability study was not previously performed. The results demonstrate the feasibility of this approach, which requires an electrophysiology recording system (allowing bipolar configuration and appropriate filtering) and some tools to insulate the guidewire, reducing the effective electrode size. The use of electrically insulated guidewires (already available in the context of biventricular device implantation) could further simplify the technique by removing the need to use a microcatheter (or an over-the-wire balloon) for insulation.

These segment-by-segment preliminary results (if confirmed in appropriately designed prospective studies comparing intracoronary mapping with other established imaging techniques in terms of revascularization decision making and patient outcome) could contribute to changing the role of the PCI guidewire from simple support for the balloon to a real-time source of useful information on myocardial structure and function.

TABLE 3 Performance of the Peak-to-Peak Voltage of the Intracoronary Electrograms for Viability Detection With Different Filter Settings at 2 Significant Operating Points

Operating Point	Filter, Hz	Cutoff, mV	Sensitivity, %	Specificity, %
Minimal value of the viable group distribution	HP-0.5	2.4	100	22
	HP-30	0.92	100	18
	HP-100	0.73	100	64
Optimal operating point*	HP-0.5	4.62	92	70
	HP-30	2.21	94	79
	HP-100	0.78	99	69

*See text for details.
HP = high pass.

ACKNOWLEDGMENTS The authors thank Chiara Esposti, PhD, Silvia Gilardone, PhD, and Andrè Sakr, PhD, for their help in processing the intracoronary recordings and Alberto Maestroni, MD, for his support in DE-MRI analysis.

REPRINT REQUESTS AND CORRESPONDENCE: Dr. Ettore Petrucci, Cardiologia Interventistica, Ospedale di Circolo di Busto Arsizio, Piazzale Prof. G. Solaro 3, 21052 Busto Arsizio (Va), Italy. E-mail: epetrucci@aobusto.it.

REFERENCES

1. Allman KC, Shaw LJ, Hachamovitch R, Udelson JE. Myocardial viability testing and impact of revascularization on prognosis in patients with coronary artery disease and left ventricular dysfunction: a meta-analysis. J Am Coll Cardiol 2002;39:1151–8.

2. Camici PG, Prasad SK, Rimoldi OE. Stunning, hibernation, and assessment of myocardial viability. Circulation 2008;117:103–14.

3. Gerber BL, Rousseau MF, Ahn SA, et al. Prognostic value of myocardial viability by delayed-enhanced magnetic resonance in patients with coronary artery disease and low ejection fraction. J Am Coll Cardiol 2012;59:825–35.

4. Yancy CW, Jessup M, Bozkurt B, et al. 2013 ACCF/AHA Guideline for the Management of Heart Failure. J Am Coll Cardiol 2013;62:e147–239.

5. Schinkel AF, Bax JJ, Boersma E, et al. Assessment of residual myocardial viability in regions with chronic electrocardiographic Q-wave infarction. Am Heart J 2002;144:865–9.

6. Yang H, Pu M, Rodriguez D, et al. Ischemic and viable myocardium in patients with non-Q-wave or Q-wave myocardial infarction and left ventricular dysfunction: a clinical study using positron emission tomography, echocardiography, and electrocardiography. J Am Coll Cardiol 2004;43:592–8.

7. Wu KC, Lima JAC. Noninvasive imaging of myocardial viability. Circ Res 2003;93:1146–58.

8. Wrobleski D, Houghtaling C, Josephson ME, et al. Use of electrocardiogram characteristics during sinus rhythm to delineate the endocardial scar in a porcine model of healed myocardial infarction. J Cardiovasc Electrophysiol 2003;14:524–9.

9. Callans DJ, Ren JF, Michele J, et al. Electroanatomic left ventricular mapping in the porcine model of healed anterior myocardial infarction: correlation with intracardiac echocardiography and pathological analysis. Circulation 1999;100:1744–50.

10. Codreanu A, Odille F, Aliot E, et al. Electroanatomic characterization of post-infarct scars. Comparison with 3-dimensional myocardial scar reconstruction based on magnetic resonance imaging. J Am Coll Cardiol 2008;52:839–42.

11. Botker HE, Lassen JF, Hermansen F, et al. Electromechanical mapping for detection of myocardial viability in patients with ischemic cardiomyopathy. Circulation 2001;103:1631–7.

12. Koch KC, vom Dhal J, Wenderdel M, et al. Myocardial viability assessment by endocardial electroanatomic mapping: comparison with metabolic imaging and functional recovery after coronary revascularization. J Am Coll Cardiol 2001;38:91–8.

13. Vahlhaus C, Bruns HJ, Stypmann J, et al. Direct epicardial mapping predicts the recovery of left ventricular dysfunction in chronic ischemic myocardium. Eur Heart J 2004;25:151–7.

14. Soejima K, Stevenson WG, Sapp JL, et al. Endocardial and epicardial radiofrequency ablation of ventricular tachycardia associated with dilated cardiomyopathy: the importance of low voltage scars. J Am Coll Cardiol 2004;43:1834–8.

15. Cerqueira MD, Weissman NJ, Dilsizian V, et al. Standardized myocardial segmentation and nomenclature for tomographic imaging of the heart. Circulation 2002;105:539–42.

16. Blancherd SM, Damlano RJ Jr., Asano T, et al. The effects of distant cardiac electrical events on local activation in unipolar epicardial electrograms. IEEE Trans Biomed Eng 1987;34:539–46.

17. Desjardins B, Morady F, Bogun F. Effect of epicardial fat on electroanatomical mapping and epicardial catheter ablation. J Am Coll Cardiol 2010;56:1320–7.

18. Heiberg E, Sjögren J, Ugander M, et al. Design and validation of Segment–a freely available software for cardiovascular image analysis. BMC Medical Imaging 2010;10:1.

19. Kim HW, Farzaneh-Far A, Kim RJ. Cardiovascular magnetic resonance in patients with myocardial infarction. J Am Coll Cardiol 2010;55:1–16.

20. Stevenson WG, Soejima K. Recording techniques for clinical electrophysiology. J Cardiovasc Electrophysiol 2005;16:1017–22.

21. Ortiz-Pérez JT, Rodríguez J, Meyers SN, et al. Correspondence between the 17-segment model and coronary arterial anatomy using contrast-enhanced cardiac magnetic resonance imaging. J Am Coll Cardiol Img 2008;3:282–93.

22. Meier B, Rutishauser W. Coronary pacing during percutaneous transluminal coronary angioplasty. Circulation 1985;71:557–61.

23. Balian V, Galli M, Repetto S, et al. Intracoronary ST segment evolution during primary coronary stenting predicts infarct zone recovery. Cathet Cardiovasc Interv 2005;64:53–60.

24. Yajima J, Saito S, Honye J, et al. Intracoronary electrocardiogram for early detection of myocardial viability during coronary angioplasty in acute myocardial infarction. Int J Cardiol 2001;79:293–9.

25. Abaci A, Oguzhan A, Topsakal R, et al. Intracoronary electrogram and angina pectoris during percutaneous coronary interventions as an assessment of myocardial viability: comparison with low-dose dobutamine echocardiography. Cathet Cardiovasc Interv 2003;60:469–76.

26. Balian V, Galli M, Marcassa C, et al. Intracoronary ST-segment shift soon after elective percutaneous coronary intervention accurately predicts periprocedural myocardial injury. Circulation 2006;114:1948–54.

27. Uetani T, Amano T, Kumagai S, et al. Intracoronary electrocardiogram recording with a bare-wire system: perioperative ST-segment elevation in the intracoronary electrocardiogram is associated with myocardial injury after elective coronary stent implantation. J Am Coll Cardiol Intv 2009;2:127–35.

28. Balian V, Marcassa C, Galli M, et al. Intracoronary electrocardiogram ST segment shift evaluation during intravenous adenosine infusion: a comparison with fractional flow reserve. Cardiol J 2011;18:662–7.

29. Meier P, Gloekler S, Zbinden R, et al. Beneficial effect of recruitable collaterals. A 10 year follow-up study in patients with stable coronary artery disease undergoing quantitative collateral measurements. Circulation 2007;116:975–83.

30. Kumagai K, Takahashi A, Yamauchi Y, Aonuma K. Ventricular tachycardia originating from the epicardium identified by intracoronary mapping using a PTCA guidewire. J Cardiovasc Electrophysiol 2006;17:670–3.

KEY WORDS angioplasty, electrocardiography, revascularization, viability